

# RSC Advances



This is an *Accepted Manuscript*, which has been through the Royal Society of Chemistry peer review process and has been accepted for publication.

*Accepted Manuscripts* are published online shortly after acceptance, before technical editing, formatting and proof reading. Using this free service, authors can make their results available to the community, in citable form, before we publish the edited article. This *Accepted Manuscript* will be replaced by the edited, formatted and paginated article as soon as this is available.

You can find more information about *Accepted Manuscripts* in the [Information for Authors](#).

Please note that technical editing may introduce minor changes to the text and/or graphics, which may alter content. The journal's standard [Terms & Conditions](#) and the [Ethical guidelines](#) still apply. In no event shall the Royal Society of Chemistry be held responsible for any errors or omissions in this *Accepted Manuscript* or any consequences arising from the use of any information it contains.

Cite this: DOI: 10.1039/c0xx00000x

www.rsc.org/xxxxxx

PAPER

# Biodegradable multiblock polyurethane micelles with tunable reduction-sensitivity for on-demand intracellular drug delivery

Xueling He,<sup>‡a</sup> Mingming Ding,<sup>‡b</sup> Jiehua Li,<sup>b</sup> Hong Tan,<sup>\*b</sup> Qiang Fu<sup>b</sup> and Liang Li<sup>\*a</sup>

Received (in XXX, XXX) Xth XXXXXXXXXX 20XX, Accepted Xth XXXXXXXXXX 20XX

DOI: 10.1039/b000000x

Redox-responsive nanovehicles containing disulfide bonds are particularly promising for targeted intracellular drug delivery. However, conventional reduction-sensitive nanocarriers generally lack control of stimuli-responsiveness due to their poor structural tunability. In this study, we developed a class of biodegradable multiblock polyurethanes bearing varied amounts of disulfide linkages in their backbone. The reducible polyurethanes exhibit interesting phase behavior and self-assembly properties, as well as triggered release profiles under intracellular reduction-mimicking environment. It was found that the redox-sensitive polyurethane micelles can rapidly enter tumor cells and efficiently transport the encapsulated payloads into the cytosol. *In vitro* cytotoxicity studies demonstrated that the paclitaxel-loaded polyurethane micelles could inhibit the proliferation of tumor cells effectively, with the inhibition effects controlled by adjusting the disulfide content in the polymeric backbone. In addition, the drug-free nanomicelles possess good cytocompatibility toward both cancer cells and healthy cells. These multiblock bioresponsive polyurethanes hold great promise in the further development of controllable intracellular drug transporters.

## Introduction

Nanoscale drug delivery systems have shown prolonged circulation time in the bloodstream and passive accumulation in vascularized solid tumors owing to the enhanced permeability and retention (EPR) effect. However, low antitumor efficacy, severe toxic side effects, and potential multiple drug resistance (MDR) still remain major challenges in cancer chemotherapy. To address these issues, bioresponsive nanomedicines that display temporarily high stability in circulation and triggered release of therapeutics at pathological sites in response to specific stimulus hold great promise for on-demand drug dosing and effective antitumor drug delivery.<sup>1</sup> Redox-sensitive nanoscopic vehicles containing disulfide bonds are particularly interesting, because of the presence of redox-potential gradient between the extra- and intracellular space.<sup>2</sup> Disulfide bonds can be cleaved in the presence of reducing agents such as L-cysteine and glutathione (GSH) through thiol-disulfide exchange reactions. In humans, GSH present in millimolar concentrations (~10 mM) in the cytosol, whereas it is found at micromolar concentrations (approximately ~2 μM) in the blood plasma due to rapid enzymatic degradation.<sup>3</sup> Interestingly, the cytosolic GSH concentration in some tumor cells has been found about several times higher than that in normal cells.<sup>4</sup> Therefore, drug delivery based on disulfide functionality can facilitate targeted and intracellular transport of the encapsulated therapeutics by cleavage of this bond.

In recent years, a great deal of redox-sensitive polymer nanoparticles have been developed, introducing disulfide linkages into the backbone<sup>5-10</sup> and side chains<sup>11,12</sup> of biodegradable

polymeric materials or using reducible crosslinkers,<sup>13-23</sup> for efficient delivery of antitumor drugs into tumor cells. In particular, the polymers bearing disulfide linkages in the backbone are especially interesting, as the cleavage of disulfide bond may result in the break of polymer main chain or the detachment of micellar shell, which usually result in the disintegration of polymer nanocarriers. To date, most studies on redox-sensitive vehicles have focused on diblock or triblock copolymers containing a single disulfide linkage between hydrophobic and hydrophilic blocks.<sup>24-28</sup> For example, Zhong et al.<sup>26</sup> reported a diblock copolymer based on disulfide linked poly(ethylene glycol)-b-poly(ε-caprolactone) (PEG-SS-PCL). They first synthesized a PCL diol bearing disulfide bond (PCL-SS-PCL) through ring-opening polymerization of ε-caprolactone (ε-CL) using bis(2-hydroxyethyl)disulfide as an initiator and stannous octoate as a catalyst, followed by the cleavage of disulfide bond by using reducing agent and catalyst to yield mercapto PCL (PCL-SH). Meanwhile, another series of reactions were carried out to prepare PEG-SH and PEG orthopyridyl disulfide (PEG-SS-Py). Finally, the PEG-SS-PCL was obtained *via* the exchange reaction between PEG-SS-Py and PCL-SH. The synthetic process of disulfide-containing copolymers needing multi-step reactions seems relatively complex. In addition, the nanocarriers based on traditional diblock or triblock copolymers have been shown to suffer from their poor structural tunability.<sup>29</sup> Therefore, mixed micelles or multicomponent systems have attracted considerable attention for providing more control over micellization and responsiveness or incorporating extra

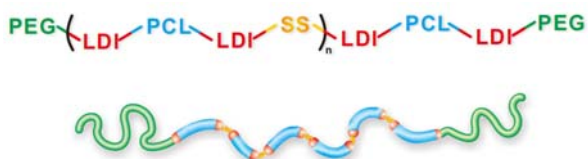


**Fig. 1.** Schematic molecular structure of reduction-sensitive multiblock polyurethanes. SS represents the chain extender DHDS.

5 functionality.<sup>30-32</sup>

Recently, we have used multiblock polyurethane as a platform to fabricate pH-sensitive and redox-responsive nanocarriers for smart drug delivery.<sup>33-36</sup> The good biocompatibility, facile preparation and highly tunable character of polyurethanes enable the incorporation of different hydrophobic/hydrophilic segments and functional groups into the polymer chains to construct multifunctional drug delivery systems.<sup>37-39</sup> Herein, we develop a class of biodegradable multiblock polyurethanes with tunable reduction-sensitivity *via* a facile and economic procedure. The amount of disulfide linkages in the polymeric backbone was easily controlled by virtue of the excellent molecular tailorability of polyurethanes (Fig. 1). The bulk properties, self-assembly, stability and stimuli-responsiveness of polyurethanes were fully characterized. Paclitaxel (PTX) was chosen as a model anticancer drug to evaluate the loading and triggered release behaviors. In addition, confocal laser scanning microscopy (CLSM) and methyl tetrazolium (MTT) assay were carried out to investigate the *in vitro* cellular uptake and intracellular drug release, antitumor activity, as well as cytocompatibility of reduction-sensitive polyurethane micelles.

## Experimental section

### Materials

*N,N*-dimethylacetamide (DMAc) was dried over CaH<sub>2</sub>, vacuum distilled, and stored in the presence of 4Å molecular sieves. PEG ( $M_n = 1900$ , Alfa Aesar, UK) and PCL ( $M_n = 2000$ , Dow Chemical, USA) were dehydrated under reduced pressure at 90 °C for 2 h before use. L-Lysine ethyl ester diisocyanate (LDI) was synthesized and purified according to previous report.<sup>37</sup> 1,4-butandiol (BDO, Fluka chemika, Switzerland) was distilled under vacuum, and bis(2-hydroxyethyl) disulfide (DHDS, Alfa Aesar) was used as received. PTX (99.5%) was obtained from Shanghai Jinhe Bio-Technology Co., Ltd, China.

### Characterization

Gel permeation chromatography (GPC) was performed on a PL-GPC 220 (Polymer Laboratory Ltd., England) using *N,N*-dimethyl-formamide (DMF)/LiBr as eluent and polymethyl methacrylate (PMMA) as reference. The sample concentration was 1.000 mg mL<sup>-1</sup>, and the flow rate was 1.000 mL min<sup>-1</sup>.

Proton nuclear magnetic resonance (<sup>1</sup>H NMR) spectra were recorded on a Bruker AV II-400 MHz spectrometer in DMSO-*d*<sub>6</sub> or D<sub>2</sub>O using tetramethylsilane (TMS) as an internal standard.

Fourier transform infrared (FTIR) spectra were obtained on a Nicolet 6700 spectrometer (Thermo Electron Corporation) between 4000 and 600 cm<sup>-1</sup> with a resolution of 4 cm<sup>-1</sup>.

Differential scanning calorimetry (DSC) was performed on a Perkin-Elmer Pyris Diamond DSC (Perkin-Elmer Instruments, USA) at a heating/cooling rate of 10 °C min<sup>-1</sup> in the range of -100

to 100 °C under a steady flow of nitrogen.

Transmission electron microscopy (TEM) was performed on a Hitachi model H-600-4 TEM with an accelerating voltage of 75 KV. A drop of micellar solution stained by 1% (w/v) phosphotungstic acid was placed on a copper grid with Formvar film, and then the liquid was blotted off and air-dried before measurement.

Sizes and zeta potentials of polyurethane nanomicelles were measured with a Zetasizer Nano ZS dynamic light-scattering (DLS) instrument (Malvern, UK) at 25 °C at an angle of 90°.

Fluorescence measurements were performed on a 970 CRT fluorescence spectrophotometer (Shanghai precision & scientific instrument Co., Ltd., China). As a hydrophobic probe, certain amounts of pyrene in acetone were added into a series of vials. After acetone was evaporated, each vial was added micellar solution with different concentrations. The final concentration of pyrene was 5.0 × 10<sup>-7</sup> M. All samples were immersed in a sonicator for 4 h at room temperature. Steady-state fluorescence spectra were recorded with bandwidths of 5.0 nm for excitation and 2.0 nm for emission, respectively. The excitation spectra ( $\lambda_{em} = 372.0$  nm) were collected, and the intensity ratio of the peak at 337.0 nm to that at 333.5 nm from excitation spectra is plotted against the log of the micelle concentration. Critical micelle concentrations (CMCs) were calculated according to the plot.

### Synthesis of reduction-sensitive polyurethanes

Reduction-sensitive multiblock polyurethanes were synthesized from LDI, PCL, BDO, DHDS and MPEG *via* a multi-step solution polymerization in DMAc (Fig. S1), with feed ratios shown in Table 1. PCL (4 g) and LDI (1.19 g) were dissolved in 25 mL DMAc and reacted at 60 °C for 1 h under a dry nitrogen atmosphere. Then BDO and DHDS with different molar ratios as chain extenders and 1‰ stannous octoate as a catalyst were added, and the reaction was kept at 65 °C for 3 h. Afterward, MPEG (1.9 g) was added and the reaction was continued at 60 °C and 85 °C for 1 and 5 h, respectively. The resultant solutions are precipitated in a mixture of methanol and diethyl ether and dried under vacuum at 60 °C for 48 h.

### Preparation of polyurethane micelles

Reduction-sensitive polyurethane micelles were prepared by a dialysis method. Briefly, 2.5 mL of polymer solution in DMAc was added dropwise to 10 mL of deionized water. The solution was then transferred to a dialysis tube (MWCO 3500) and dialyzed against deionized water for about 3 days to remove the organic solvent at room temperature. The micelle solution was centrifugalized at 3000 r min<sup>-1</sup> for 10 min and passed through a 0.45 μm pore-sized syringe filter (Milipore, Carrigtwohill, Co. Cork, Ireland).

### Stability and reductive degradation of polyurethane micelles

GSH (10 mM) was added into the micellar solutions to simulate the intracellular reduction environment within tumor cells. The changes of size and size distributions of micelles in response to GSH were measured at different time intervals. The degradation products obtained by 24-h incubation in 10 mM of GSH at 37 °C were lyophilized for DSC analysis.

### Drug loading and release

**Table 1** Characteristics of reduction-sensitive multiblock polyurethanes and their micelles.

Samples <sup>a</sup>	Feed ratio (mol)					Molecular Weights <sup>b</sup>			Size (nm)	Pdl	Zeta potential (mV)
	LDI	PCL	MPEG	BDO	DHDS	M <sub>n</sub> (g mol <sup>-1</sup> )	M <sub>w</sub> (g mol <sup>-1</sup> )	M <sub>w</sub> /M <sub>n</sub>			
SS0	2	0.8	0.4	1.0	0	19000	22500	1.19	91.4 ± 1.39	0.08 ± 0.02	-16.2 ± 0.85
SS30	2	0.8	0.4	0.7	0.3	18200	22900	1.26	99.9 ± 1.45	0.28 ± 0.01	-23.0 ± 0.67
SS50	2	0.8	0.4	0.5	0.5	16700	21200	1.27	110.0 ± 1.00	0.22 ± 0.01	-23.1 ± 1.01
SS70	2	0.8	0.4	0.3	0.7	22800	30800	1.35	57.7 ± 0.10	0.22 ± 0.01	-14.5 ± 2.49
SS100	2	0.8	0.4	0	1.0	19500	26200	1.34	86.4 ± 0.21	0.19 ± 0.01	-16.7 ± 0.64

<sup>a</sup> Reduction cleavable polyurethanes are denoted as SSX, where SS is for DHDS, X is the molar content of DHDS in chain extender. <sup>b</sup> Molecular weights and molecular weight distributions were determined by GPC.

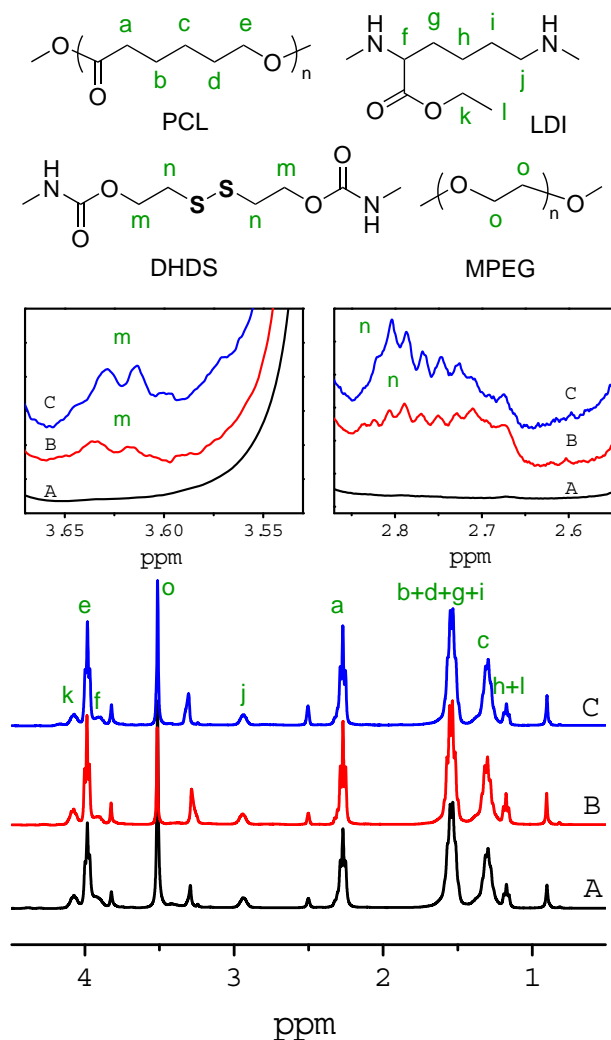


**Fig. 2.** 400 MHz <sup>1</sup>H NMR spectra of reduction-sensitive polyurethanes in DMSO-*d*<sub>6</sub>: (A) SS0, (B) SS50 and (C) SS100.

PTX as a model drug was loaded into reduction-sensitive polyurethane nanomicelles by a micelle extraction technique. A measured amount of drug stock solution (5 mg mL<sup>-1</sup>) in acetone was added to the empty vial, and the solvent was evaporated under nitrogen. Then 10 mL of micelle solution was transferred into the vial and ultrasonated for 2 h. The solution was centrifugalized at 3000 r min<sup>-1</sup> for 10 min and passed through a 0.45 μm pore-sized syringe filter (Millipore, Carrigtwohill, Co. Cork, Ireland) to remove any insoluble drug. The amount of drugs loaded inside micelles was determined by a model LC-6A high-performance liquid chromatography (HPLC) system (Shimadzu,

Kyoto, Japan) equipped with a reverse-phase C18 column (4.6 × 250 mm, 5 μm) and an SPD-6AV detector. The flow rate was 1.0 mL min<sup>-1</sup>, and the mobile phase consisted of acetonitrile/water (60/40 v/v). The detection of PTX was performed by UV absorption at 227 nm. The loading content (%) and encapsulation efficiency (%) were calculated based on the equations below:

Loading content (LC) (%) = mass of drugs in micelles / total mass of loaded micelles × 100%

Encapsulation efficiency (EE) (%) = mass of drugs in micelles / initial amount of feeding drugs × 100%.

The release of PTX was conducted using a dialysis method. 2.5 mL of micelle solution (1 mg mL<sup>-1</sup>) loading 4.8% of PTX was placed into a dialysis tube (MWCO 3500), and dialyzed against 25 mL phosphate buffer solution (PBS, 10 mM, pH 7.4) with or without 10 mM GSH at 37 °C in a water bath with shaking. The release media also contains 100 mM sodium salicylate to maintain a sink condition.<sup>52</sup> At desired time intervals, 2 mL of release media was sampled and replenished with an equal volume of fresh media. The release experiments were conducted in triplicate. The PTX concentration was determined with HPLC.

#### 40 Cell culture

Human liver cell line HepG2 was cultured in RPMI 1640 medium supplemented with 2 mM L-Glutamine, 100 U mL<sup>-1</sup> penicillin and 10% fetal bovine serum (FBS) (FBS, Hyclone, Logan, UT) at 37 °C in a humidified atmosphere containing 5% CO<sub>2</sub> (Sanyo Incubator, MCO-18AIC, Japan).

3T3 mouse fibroblasts were maintained in Dulbecco's modified Eagle's medium (DMEM, Gibco Life, Grand Island, NY, USA) supplemented with 10% (v/v) fetal bovine serum (FBS, Hyclone, Logan, UT), 2 mM L-glutamine and 1% (v/v) antibiotics mixture (10,000U of penicillin and 10 mg of streptomycin) (Gibco). The cells were incubated in a humidified atmosphere of 5% CO<sub>2</sub> at 37 °C (Sanyo Incubator, MCO-18AIC, Japan).

#### Cellular uptake and intracellular release of payloads

Confocal laser scanning microscopy (CLSM) was employed to examine the cellular uptake and intracellular release behaviors of polyurethane micelles. The micelles were labeled with fluorescein isothiocyanate isomer I (FITC, 90%, Acros Organics) and incubated with HepG2 cells for 1 h at 37 °C. After removal of the medium, the cells were washed three times with cold PBS, fixed with 1 mL of 4% paraformaldehyde for 30 min at 4 °C, and stained with 2-(4-amidinophenyl)-6-indolecarbamidine dihydrochloride (DAPI, Roche) for 10 min. Finally, the slides were mounted with 10% glycerol solution and observed by a Leica TCS SP5 (Leica Microscopy Systems Ltd., Germany).

#### 65 Cell viability assay

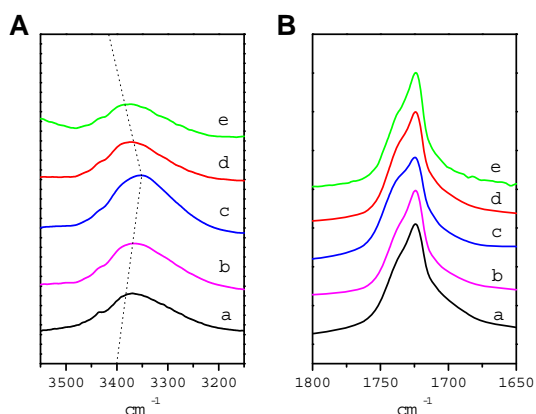


**Fig. 3.** FTIR spectra in the (A) NH and (B) C=O stretching regions of reduction-sensitive biodegradable multiblock polyurethanes: (a) SS0, (b) SS30, (c) SS50, (d) SS70 and (e) SS100.

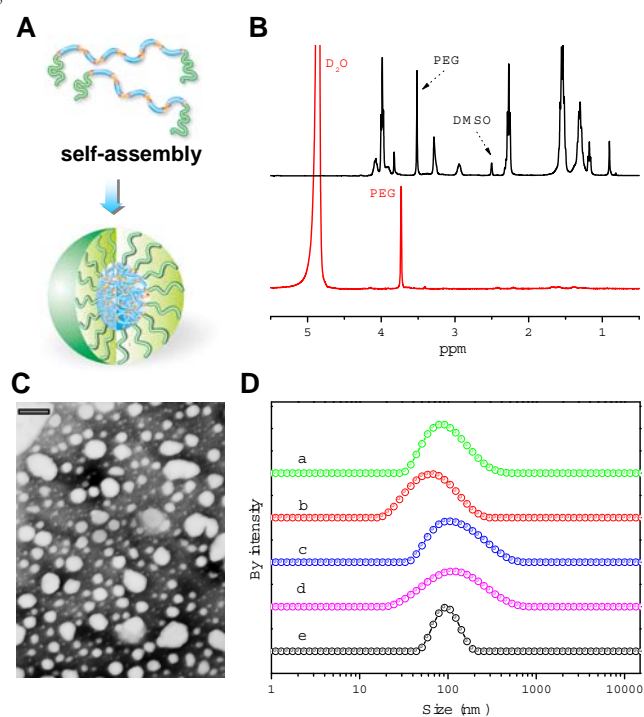


**Fig. 4.** (A) Schematic illustration of the self-assembly of reduction-sensitive multiblock polyurethanes. (B) <sup>1</sup>H NMR spectra of reduction-sensitive polyurethane in DMSO-*d*<sub>6</sub> and its micelles in D<sub>2</sub>O. (C) TEM micrographs of reduction-sensitive polyurethane micelles. Scale bar: 100 nm. (D) Size distributions of reduction-sensitive polyurethane micelles determined by DLS: (a) SS0, (b) SS30, (c) SS50, (d) SS70 and (e) SS100.

To evaluate the antitumor activity of PTX-loaded polyurethane micelles and cytocompatibility of drug-free micelles, HepG2 cells and 3T3 mouse fibroblasts were seeded in 96-well plates at  $1 \times 10^3$  cells/well and incubated for 24 h. The culture medium was removed and replaced with 100  $\mu$ L medium containing various concentrations of micelle solutions for another 24 h of incubation. Then 20  $\mu$ L of 3-(4,5-dimethylthiazol-2-yl)-2,5-diphenyl tetrazolium bromide (MTT) solution (5 mg mL<sup>-1</sup>, Sigma) was added to each well. After incubating the cells for 4 h, the MTT solution was removed and the insoluble formazan crystals were

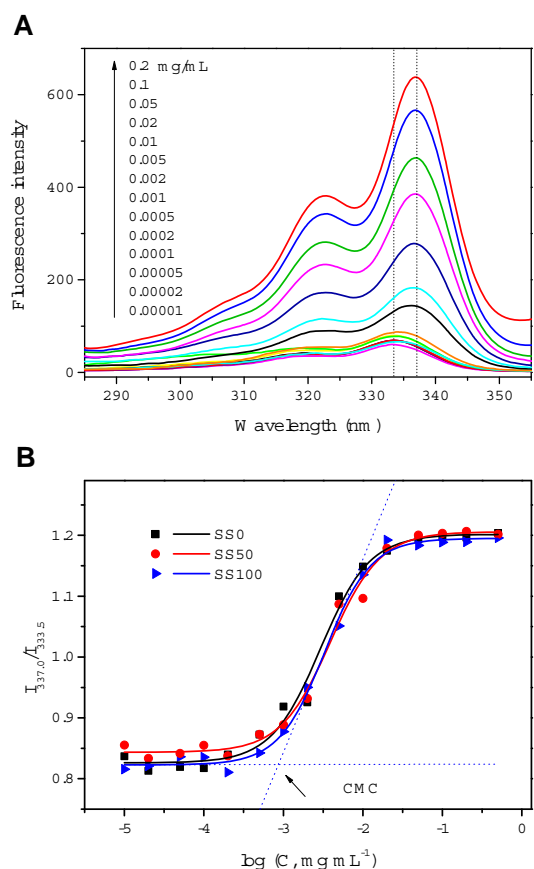


**Fig. 5.** (A) Typical fluorescence excitation spectra ( $\lambda_{em} = 372$  nm) of reduction-sensitive polyurethane micelles. (B)  $I_{337.0}/I_{333.5}$  ratios in the excitation spectra as a function of micellar concentrations ( $\log C$ ). The CMCs are obtained from the intersection of the two tangent lines shown by the arrows.

dissolved in 100  $\mu$ L dimethyl sulfoxide (DMSO). The absorbance was measured at a wavelength of 490 nm. The cell viability was normalized to that of cells cultured in the full culture media. The dose-effect curves were plotted and the median inhibitory concentration ( $IC_{50}$ ) was determined using the software GraphPad Prism 5 for Windows (GraphPad Software, Inc., San Diego, CA).

### Statistics

Statistical analysis was carried out using the Statistical Package for the Social Sciences (SPSS, Version 17) software. Data are expressed as means  $\pm$  standard deviations (SD). The significance of difference was analyzed by one or two-way analysis of variance (ANOVA) at 95% confidence levels ( $P < 0.05$ ).

## Results and discussion

### Synthesis of reduction-sensitive polyurethanes

A series of biodegradable multiblock polyurethanes bearing disulfide linkages were synthesized from PCL, LDI, DHDS and MPEG via a facile solution polymerization. The structures of the polymers are illustrated in Fig. 1, where the amount of disulfide bonds could be easily controlled by changing the feed ratios, as shown in Table 1. The resultant polyurethanes are named SSX, where SS represents DHDS, and X is for the molar content of

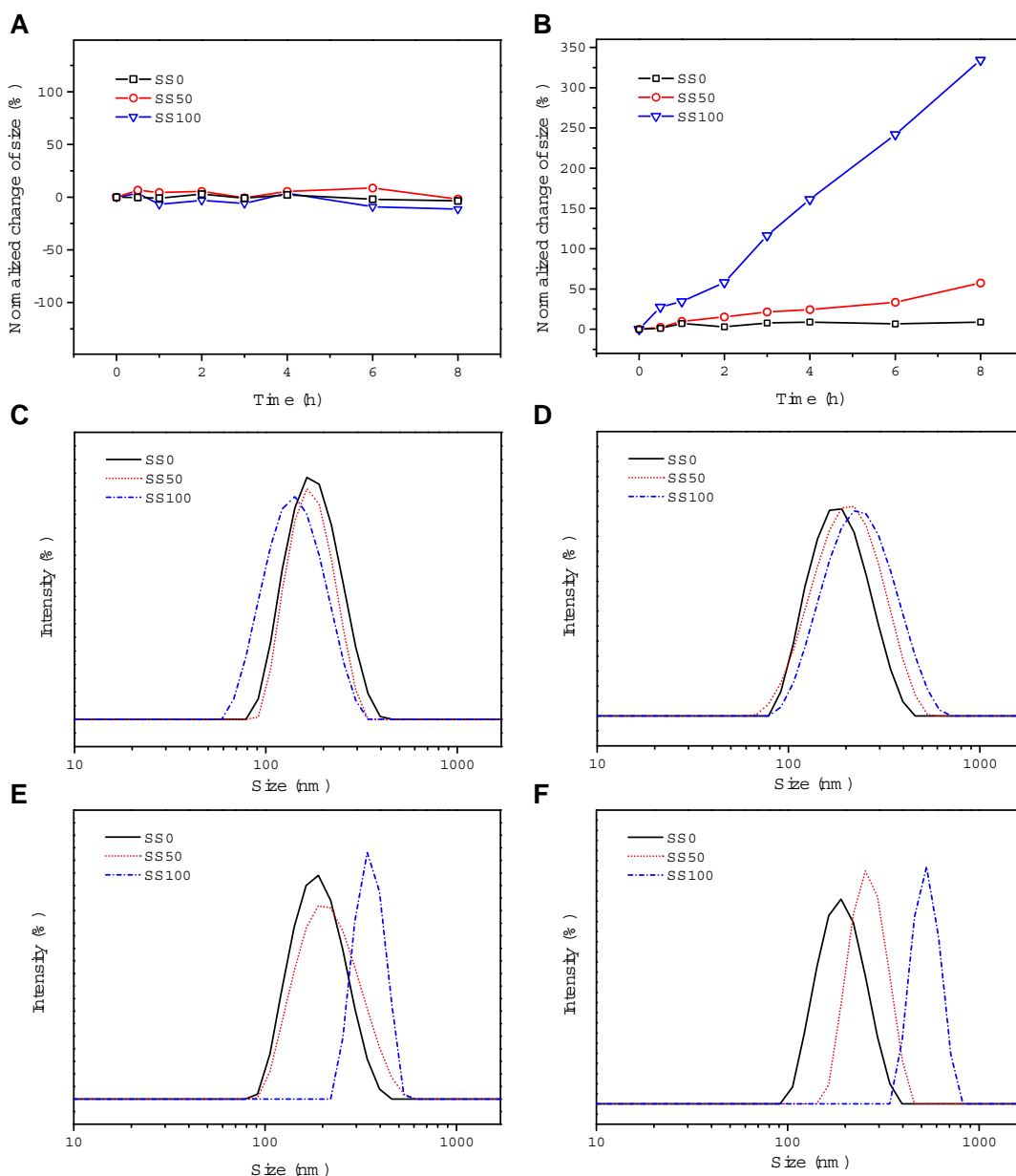


**Fig. 6.** Change in size (A, B) and size distributions (C-F) of polyurethane micelles under physiological conditions in the absence of reducing agents (A) and in the presence of 10 mM GSH (B-F) at different times: (C) 0 h, (D) 2 h, (E) 4 h, and (F) 8 h.

5 DHDS in chain extender. The molecular weights of multiblock polyurethanes determined with GPC are in the range of 16000-23000 g mol<sup>-1</sup> (Table 1), with monodisperse and narrow molecular weight distributions (Table 1 and Fig. S2), which are appropriate for using as drug carriers.

10 The <sup>1</sup>H NMR spectra of reductive polyurethanes are presented in Fig. 2. The peaks at 3.98 (-CH<sub>2</sub>O-), 2.27 (-CH<sub>2</sub>COO-), 1.55 (-CH<sub>2</sub>CH<sub>2</sub>CH<sub>2</sub>-) and 1.31 ppm (-CH<sub>2</sub>CH<sub>2</sub>CH<sub>2</sub>-) are attributed to the methylene protons of PCL unit. The signal at 3.51 ppm is assigned to the methylene protons of PEG block (-CH<sub>2</sub>CH<sub>2</sub>O-). The chemical shifts of methylene and methyl protons in the ethoxyl group of LDI are found at 4.07 (-CH<sub>2</sub>OCO-) and 1.17 ppm (-CH<sub>3</sub>), respectively, suggesting the successful synthesis of PCL/LDI/PEG-based urethane copolymers. In addition, two triplets observed at 2.80 and 3.60

20 ppm are derived from the hydrogen atoms in  $\alpha$ -methylene (-S-CH<sub>2</sub>) and  $\beta$ -methylene (-S-CH<sub>2</sub>-CH<sub>2</sub>) next to the disulfide bond, respectively. These signals are found strengthened with the increase of DHDS content in chain extender, demonstrating that the designed amount of disulfide linkages have been successfully

25 incorporated into the backbone of polyurethanes.

The FTIR spectra of polyurethanes are shown in Figs. 3 and S3. A broad stretching band around 3350 cm<sup>-1</sup> is mainly attributed to the N-H stretching vibration, while the stretching band in the 1600-1800 cm<sup>-1</sup> region is overlapped by the absorption of ester carbonyl groups of PCL, free and hydrogen-bonded carbonyl of urethane groups. The absorption peaks at 2940 and 2870 cm<sup>-1</sup> are corresponded to the stretching vibration of methyl and methylene, respectively. The peaks at 1250 and 1050 cm<sup>-1</sup> belong to C-O-C symmetric and asymmetric stretching

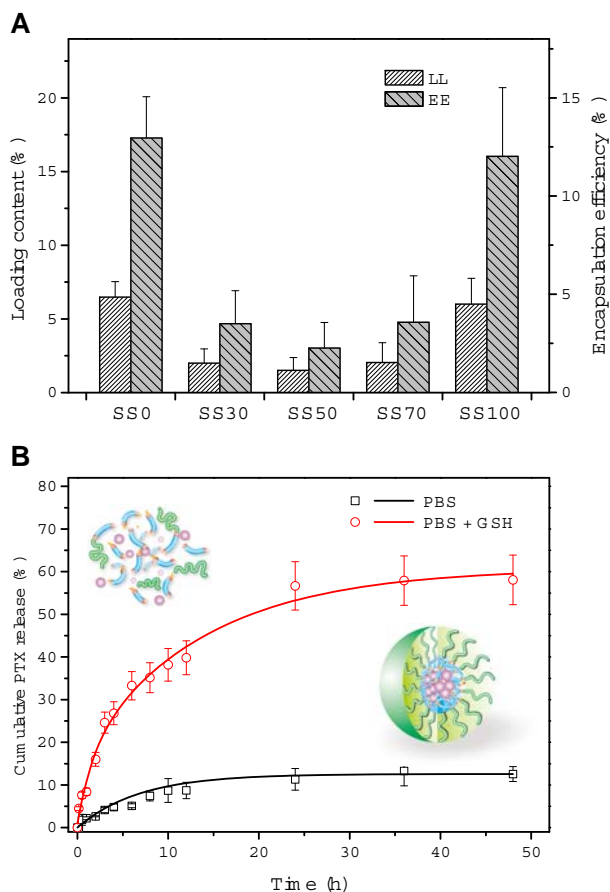


**Fig. 7.** (A) Drug loading content and encapsulation efficiency for PTX loaded in reduction sensitive polyurethane micelles. (B) Time-dependent cumulative release of PTX from reduction sensitive polyurethane micelles (SS100) in PBS buffer solutions (pH 7.4, 10 mM) with and without 10 mM of GSH.

vibration of ester, respectively. The absorption at 1100 and 1130  $\text{cm}^{-1}$  are attributed to ether group (C-O-C) stretching vibration of PEG. The FTIR results are in good agreement with  $^1\text{H}$  NMR results, indicating that all the desired blocks are successfully copolymerized into multiblock polyurethanes. Interestingly, with the increase of disulfide amount in polyurethane structure, a red shift of N-H stretching band from 3370  $\text{cm}^{-1}$  to 3352  $\text{cm}^{-1}$  occurs, followed by a blue shift to 3373  $\text{cm}^{-1}$  (Fig. 3A). Meanwhile, the signal of C=O stretching band corresponding to the free carbonyl groups ( $\sim 1720 \text{ cm}^{-1}$ ) decreases firstly and then increases with disulfide incorporation (Fig. 3B). These results reveal that the microphase separation between the hard segment and soft segment is enhanced with incorporation of small amount of disulfide linkages into the hard segment of polyurethanes, but further decreased with more disulfide bonds introduced.<sup>40</sup>

To better understand the bulk property, DSC measurement was carried out to investigate the thermal behavior of polyurethanes. The glass transition temperatures ( $T_g$ ) of soft segment, known as an indicator of the degree of phase separation,<sup>40,41</sup> is shown in Fig. S4 and listed in Table S1. Evidently, with disulfide incorporation, the  $T_g$ s of polyurethanes decrease firstly and then increase slightly. Moreover, the melting temperatures during the first and second heating and the

calculated crystallinity display a similar trend compared with  $T_g$ s (Table S1). These results agree well with FTIR analysis, further demonstrating that the introduction of different amounts of disulfide linkages may play an important role in the phase behavior and crystallization properties of multiblock polyurethanes. However, more work is needed to better understand these interesting phenomena.

### Preparation of polyurethane micelles

Like conventional diblock and triblock copolymers, the redox-responsive multiblock polyurethanes can easily self-assemble in an aqueous solution to form a micellar structure, where PCL segments confer a hydrophobic core to encapsulate water-insoluble drugs, and PEG chains form an outer corona to stabilize the micelles in blood circulation and reduces uptake at reticuloendothelial sites (Fig. 4A). The core-shell structure of polyurethane micelles was first confirmed with  $^1\text{H}$  NMR. As seen from Fig. 4B, all the characteristic peaks of PCL, LDI and MPEG are clearly detected in  $\text{DMSO-}d_6$  and in good agreement with the molecular structure of polyurethane. However, the resonance of PCL is significantly weakened and that of PEG (3.74 ppm) is greatly enhanced in  $\text{D}_2\text{O}$ . This result proves the formation of multiblock polyurethane nanomicelles. Another evidence of micelle formation comes from the fluorescence excitation spectrum of polyurethane solutions containing pyrene as a probe (Fig. 5A), where the (0, 0) band shifts from 333.5 to 337.0 nm with an increase of polyurethane concentration. The result demonstrates that pyrene molecules are transferred from an aqueous environment to a hydrophobic core as the micelle was formed in water.<sup>42</sup>

The sizes of polyurethane micelles determined by DLS are in the range of 57-110 nm with unimodal size distributions (Fig. 4D). All the micelles appear as well dispersed individual particles with a spherical shape, as seen from TEM image (Fig. 4C). The zeta potentials of nanoparticles in aqueous solution are listed in Table 1. Interestingly, all the micelles display negative surface charges ranging from -23.1 to -14.5 mV. Since there is no ionic group in the polymer structure, the negative zeta potential may be attributed to the delocalization of negative charges on ester bonds or the polarization of water molecules under the effect of PEG. Similar results have also been reported for micelles prepared from PEG-PCL and PCL-PEG-PLA (PLA is polylactide).<sup>43</sup> The negatively charged surface of nanomicelles may facilitate the long circulation time of drug formulations in the body.<sup>44</sup> The CMCs of polyurethane micelles were determined from the excitation spectra of pyrene (Fig. 5). The intensity of the peak at 337 nm to that at 333.5 nm is plotted against the log of polymer concentration (Fig. 5B). According to Wilhelm et al.,<sup>42</sup> the concentration dependence of the  $I_{337}/I_{333.5}$  of pyrene is sensitive to the onset of micelle aggregation. The CMC values obtained from the intersection of the two tangent lines are in the range of 6.8-9.1  $\times 10^{-4} \text{ mg mL}^{-1}$ , which are much lower than those reported for conventional diblock or triblock copolymer micelles based on PCL and PEG,<sup>45</sup> suggesting that the multiblock polyurethane micelles are thermodynamically stable.

### Stability and stimuli-responsiveness of polyurethane micelles

To further verify the stability of polyurethane nanocarriers, the micelles were incubated at 37  $^\circ\text{C}$  with gentle shaking, and the

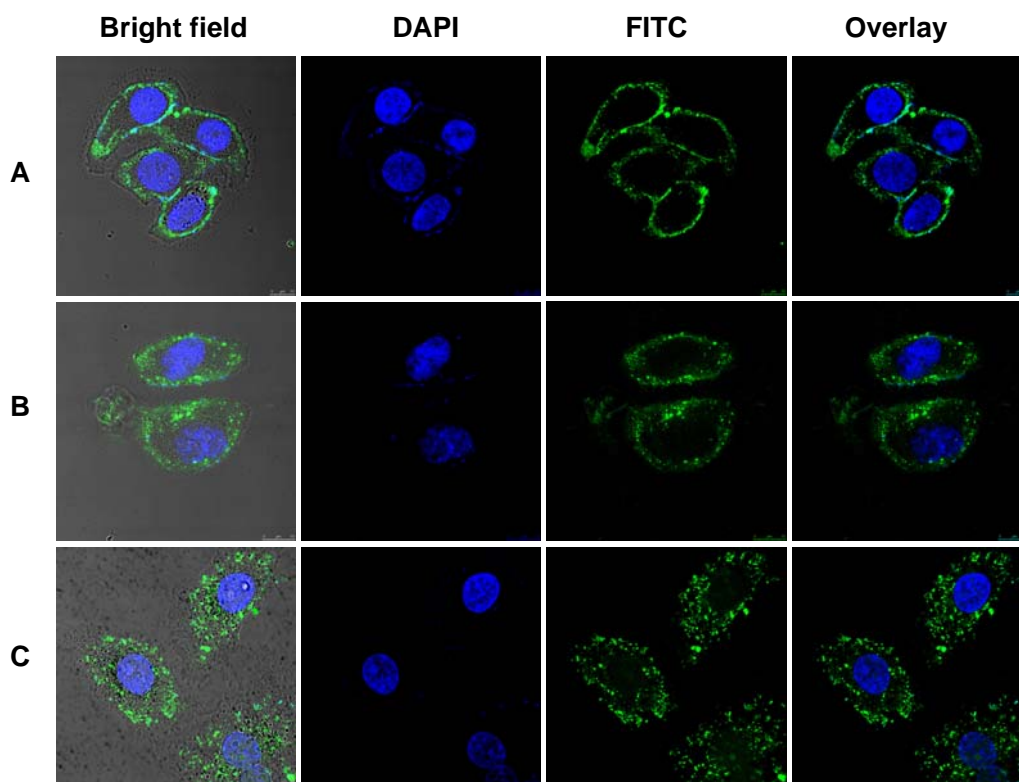


**Fig. 8.** CLSM images of HepG2 cells incubated with polyurethane micelles prepared from SS0 (A), SS50 (B) and SS100 (C) for 1 h. Polyurethane micelles were labeled with FITC (green), nuclei of cells were stained with DAPI (blue).

size was determined at different times. It was found that the micellar size and size distributions keep unchanged under a simulative physiological condition (Fig. 6A), demonstrating a good stability of polyurethane micelles. To study the potential intracellular degradation of polyurethane nanocarriers, the change of size and size distributions of micelles in response to an intracellular level of GSH was carried out. Evidently, the size of reduction-sensitive polyurethane micelles containing disulfide bonds increase dramatically in the presence of 10 mM GSH, while those of insensitive micelles remain unchanged during the time tested (Fig. 6B). This is probably due to that the reductive cleavage of disulfide bonds embedded in the polymer backbone results in the destabilization/reaggregation of polyurethane micelles. It is interesting to note that the polyurethane micelles bearing higher content of disulfide linkages undergo a greater change in size and size distributions (Fig. 6C-F), suggesting that the reduction sensitivity and degradation of polyurethanes can be well controlled by adjusting the polymeric architectures. In addition, because of the presence of biodegradable PCL units in the polymer structure, these multiblock polyurethane micelles are expected to be further degraded following the cleavage of disulfide linkages, according to our previous reports.<sup>34,37,46</sup> The two-stage degradation behavior of the reduction-sensitive polyurethane micelles will be investigated in our future work.

#### Drug loading and triggered release

To investigate the loading capacity of reductive polyurethane micelles, commercial available chemotherapeutic agent PTX was used as a model hydrophobic drug. The loading of PTX into polyurethane micelles was performed using an extraction method.

The drug loading content (LC) and encapsulation efficiency are in the range of 1.5-6.5% and 2.3-13%, respectively (Fig. 7A). These levels are comparable to those reported for traditional diblock or triblock copolymers, but lower than those obtained in our previous work.<sup>33,38b</sup> This can be attributed to the lack of gemini surfactant side chains to solubilize hydrophobic agents.

The release of PTX from polyurethane micelles was performed in a reductive environment analogous to that of intracellular compartments such as cytosol (10 mM GSH). Fig. 7B shows the release of PTX from redox-sensitive polyurethane micelles against PBS (pH 7.4) at 37 °C in the presence and absence of GSH. Notably, inefficient and slow release of PTX from SS100 micelles was observed in the absence of GSH, with only 5% PTX was released in the first 4 h and approximately 11% released within 48 h. However, in the same buffer solution with 10 mM GSH, the release of PTX was significantly accelerated, with 26% was released in 4 h and near 60% was released in 48 h, arising from the destabilization of polyurethane micelles caused by efficient disulfide cleavage. It is worth noting that the release of PTX from polyurethane micelles at earlier stage (before 24 h) was greatly faster than that over 24 h, implying that the reduction-sensitive polyurethane micelles can respond efficiently to GSH and the release of PTX may reach an equilibrium in a short period of time. These results demonstrates that the redox-responsive multiblock polyurethane nanomicelle is a highly promising drug delivery system to achieve fast intracellular release of antitumor drug.

#### Cellular uptake and intracellular release of payloads

The cellular uptake of polyurethane micelles and intracellular

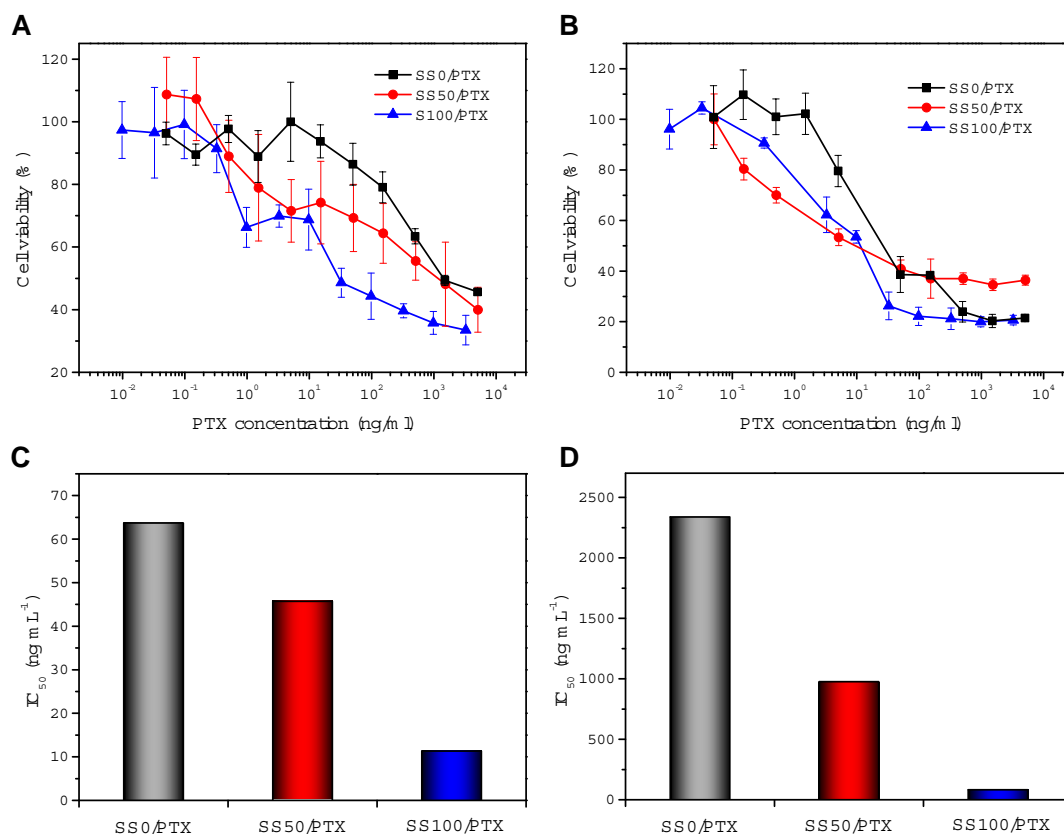


**Fig. 9.** Cytotoxicity (A, B) and IC<sub>50</sub> values (C, D) of PTX-loaded polyurethane micelles against HepG2 cells for different incubation times: (A, C) 24 h, (B, D) 72 h.

5

release of encapsulated payload from micelles was studied using CLSM in HepG2 cell line. Since PTX molecules are not fluorescent, FITC was used as an alternative to label the nanocarriers and show the intracellular release and distribution of cargoes loaded in polyurethane micelles. As shown in Fig. 8, the green fluorescence appears in all the cells after 1 h of incubation, indicating that the micelles are successfully internalized by HepG2 cells. Interestingly, different intracellular distributions of FITC fluorescence were found for polyurethane formulations with various disulfide contents. In particular, the redox-sensitive micelles display much stronger fluorescence in cytosol, possibly owing to a more efficient release of FITC molecules from micelles due to the cleavage of disulfide linkages in response to GSH in tumor cells. The result indicates that the redox-sensitive polyurethane micelles are effective vehicles to transport the payloads into the cytosol. Such a character of drug carriers is important for PTX to exert its function, because the mechanism of its action is to interfere with microtubule assembly, thus prolonging the mitotic checkpoint and causing apoptosis of tumor cells.<sup>47</sup>

### *In vitro* cytotoxicity

The cytotoxicity of PTX-loaded polyurethane micelles were subsequently determined using an MTT assay. As shown in Fig. 9, all the micellar formulations showed a time- and dose-dependent increase in cytotoxicity toward HepG2 cells. Evidently, the cytotoxicity of redox-sensitive micelles was significant higher

compared with insensitive micelles at all incubation time points. The IC<sub>50</sub> (the dose having 50% cell inhibition) of SS100/PTX micelles after 24 and 72 h incubation are 83.2 and 11.3 ng mL<sup>-1</sup>, respectively, which are significant lower than those for SS50/PTX (976.1 and 45.7 ng mL<sup>-1</sup>) and SS0/PTX (2338.0 and 63.7 ng mL<sup>-1</sup>) ( $P < 0.05$ ) (Fig. 9). The enhanced cytotoxicity of PTX-loaded redox-sensitive polyurethane micelles reveals that the reducible micelles are more potent for intracellular delivery of PTX as compared to the insensitive control. As a negative control, the cell viability of drug free micelles is above 90% even at a high concentration up to 0.1 mg mL<sup>-1</sup> (Fig. 10A, B). Furthermore, the empty micelles also do not show any inhibit effect toward 3T3 fibroblast (Fig. 10C, D). These results demonstrate that polyurethane micelles have no cytotoxicity against both cancer cells and healthy cells, and thus are fairly safe for using as pharmaceutical vehicles.

### Conclusions

In summary, we have developed a class of biodegradable multiblock polyurethanes with controlled reduction-sensitivity. The polymers bearing different amounts of cleavable disulfide linkages in the backbone can self-assemble into micelles with diameters around 100 nm, negative surface charges and low CMCs. Furthermore, the micelles display good stability under physiological condition and undergo a time- and disulfide content-dependant breakage in the presence of GSH, thus

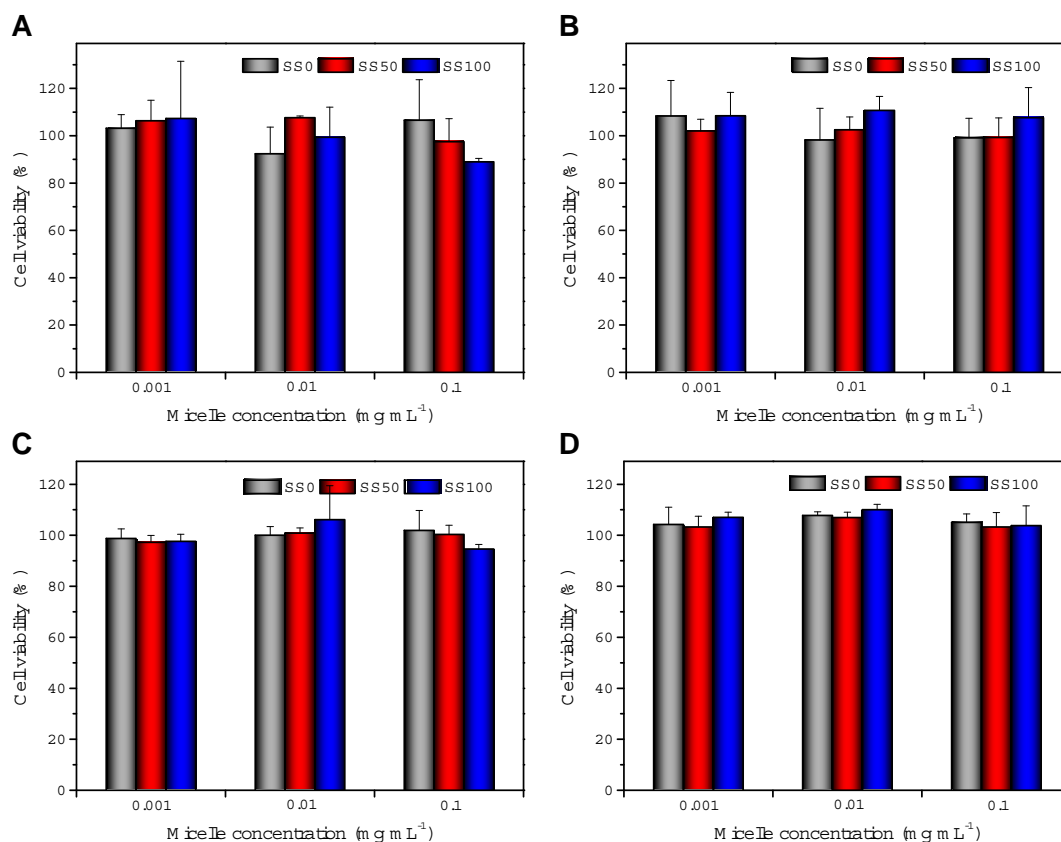


**Fig. 10.** Cell viability of HepG2 cells (A, B) and 3T3 mouse fibroblasts (C, D) after 24 h (A, C) and 72 h (B, D) of incubation with various concentrations of reduction-sensitive polyurethane micelles.

5 resulting in a triggered release of PTX from micelles. The reduction-responsive nanocarriers could rapidly internalize into HepG2 cells, and efficiently deliver the encapsulated cargoes into the cytosol. In addition, the PTX-encapsulated formulations show controlled therapeutic effects against HepG2 cells. These  
 10 nanocarriers with good biocompatibility and tunable reduction-responsiveness are promising candidates for targeted and on-demand intracellular drug delivery applications.

## Acknowledgements

Financial supports from the National Natural Science Foundation  
 15 of China (51203101, 51273126, 51073104), China Postdoctoral Science Foundation (2011M500147, 2012T50776), and Changjiang Scholars and Innovative Research Team in University (IRT1163) are acknowledged.

## Notes and references

20 <sup>a</sup> Institute of Biomedical Engineering, West China School of Preclinical and Forensic Medicine, Sichuan University, Chengdu, 610041, China. E-mail: lilianghx@163.com

<sup>b</sup> College of Polymer Science and Engineering, State Key Laboratory of Polymer Materials Engineering, Sichuan University, Chengdu 610065,  
 25 China. Fax: +86-28-8540540; Tel: +86-28-85460961; E-mail: hongtan@scu.edu.cn

† Electronic Supplementary Information (ESI) available: GPC diagrams, FTIR spectra and DSC results of reduction-sensitive polyurethanes. See DOI: 10.1039/b000000x/

30 ‡ These authors contributed equally to this work.

- 1 (a) D. Roy, J. N. Cambre and B. S. Sumerlin, *Prog. Polym. Sci.*, 2010, **35**, 278-301.; (b) H. Wei, R. Zhuo and X. Zhang, *Prog. Polym. Sci.*, 2013, **38**, 503-535.
- 2 F. Meng, W. E. Hennink and Z. Zhong, *Biomaterials*, 2009, **30**, 2180-2198.
- 3 D. P. Jones, J. L. Carlson, P. S. Samiec, P. Sternberg, V. C. Mody, R. L. Reed and L. A. S. Brown, *Clin. Chim. Acta*, 1998, **275**, 175-184.
- 4 S. Son, R. Namgung, J. Kim, K. Singha and W. J. Kim, *Accounts Chem. Res.*, 2012, **45**, 1100-1112.
- 5 L. Wong, C. Boyer, Z. Jia, H. M. Zareie, T. P. Davis and V. Bulmus, *Biomacromolecules*, 2008, **9**, 1934-1944.
- 6 A. Klaikherd, S. Ghosh and S. Thayumanavan, *Macromolecules*, 2007, **40**, 8518-8520.
- 7 M. E. H. El-Sayed, A. S. Hoffman and P. S. Stayton, *J. Controlled Release*, 2005, **101**, 47-58.
- 8 S. Son, K. Singha and W. J. Kim, *Biomaterials*, 2010, **31**, 6344-6354.
- 9 J. Ding, J. Chen, D. Li, C. Xiao, J. Zhang, C. He, X. Zhuang and X. Chen, *J. Mater. Chem. B*, 2013, **1**, 69-81.
- 10 S. Yu, C. He, J. Ding, Y. Cheng, W. Song, X. Zhuang and X. Chen, *Soft Matter*, 2013, **9**, 2637-2645.
- 11 J. Ryu, R. Roy, J. Ventura and S. Thayumanavan, *Langmuir*, 2010, **26**, 7086-7092.
- 12 J. Li, M. Huo, J. Wang, J. Zhou, J. M. Mohammad, Y. Zhang, Q. Zhu, A. Y. Waddad and Q. Zhang, *Biomaterials*, 2012, **33**, 2310-2320.
- 13 J. O. Kim, G. Sahay, A. V. Kabanov and T. K. Bronich, *Biomacromolecules*, 2010, **11**, 919-926.
- 14 Y. Li, L. Zhu, Z. Liu, R. Cheng, F. Meng, J. Cui, S. Ji and Z. Zhong, *Angew. Chem. Int. Ed.*, 2009, **48**, 9914-9918.
- 15 A. N. Koo, H. J. Lee, S. E. Kim, J. H. Chang, C. Park, C. Kim, J. H. Park and S. C. Lee, *Chem. Commun.*, 2008, 6570-6572.
- 16 X. Jiang, S. Liu and R. Narain, *Langmuir*, 2009, **25**, 13344-13350.
- 17 S. Matsumoto, R. J. Christie, N. Nishiyama, K. Miyata, A. Ishii, M. Oba, H. Koyama, Y. Yamasaki and K. Kataoka, *Biomacromolecules*,

- 2009, **10**, 119-127.
- 18 S. Yu, J. Ding, C. He, Y. Cao, W. Xu and X. Chen, *Adv. Healthcare Mater.*, DOI: 10.1002/adhm.201300308.
- 19 H. Wang, L. Tang, C. Tu, Z. Song, Q. Yin, L. Yin, Z. Zhang and J. Cheng, *Biomacromolecules*, 2013, **14**, 3706-3712.
- 20 Y. Cheng, C. He, C. Xiao, J. Ding, K. Ren, S. Yu, X. Zhuang and X. Chen, *Polym. Chem.*, 2013, **4**, 3851-3858.
- 21 L. Wu, Y. Zou, C. Deng, R. Cheng, F. Meng and Z. Zhong, *Biomaterials*, 2013, **34**, 5262-5272.
- 22 A. N. Koo, K. H. Min, H. J. Lee, S. Lee, K. Kim, I. Chan Kwon, S. H. Cho, S. Y. Jeong and S. C. Lee, *Biomaterials*, 2012, **33**, 1489-1499.
- 23 J. Yue, R. Wang, S. Liu, S. Wu, Z. Xie, Y. Huang and X. Jing, *Soft Matter*, 2012, **8**, 7426-7435.
- 24 S. Cerritelli, D. Velluto and J. A. Hubbell, *Biomacromolecules*, 2007, **8**, 1966-1972.
- 25 L. Tang, Y. Wang, Y. Li, J. Du and J. Wang, *Bioconjugate Chem.*, 2009, **20**, 1095-1099.
- 26 H. Sun, B. Guo, R. Cheng, F. Meng, H. Liu and Z. Zhong, *Biomaterials*, 2009, **30**, 6358-6366.
- 27 H. Sun, B. Guo, X. Li, R. Cheng, F. Meng, H. Liu and Z. Zhong, *Biomacromolecules*, 2010, **11**, 848-854.
- 28 (a) Y. Wang, F. Wang, T. Sun and J. Wang, *Bioconjugate Chem.*, 2011, **22**, 1939-1945.; (b) H. Wen, H. Dong, W. Xie, Y. Li, K. Wang, G. M. Pauletti and D. Shi, *Chem. Commun.*, 2011, **47**, 3550-3552.; (c) Y. Li, X. Lei, H. Dong and T. Ren, *RSC Adv.*, 2014, **4**, 8165-8176.
- 29 T. Zou, S. Li, X. Zhang, X. Wu, S. Cheng and R. Zhuo, *J. Polym. Sci., Part A: Polym. Chem.*, 2007, **45**, 5256-5265.
- 30 W. Wang, H. Sun, F. Meng, S. Ma, H. Liu and Z. Zhong, *Soft Matter*, 2012, **8**, 3949-3956.
- 31 S. C. Abeylath, S. Ganta, A. K. Iyer and M. Amiji, *Accounts Chem. Res.*, 2011, **44**, 1009-1017.
- 32 X. Xiong and A. Lavasanifar, *ACS Nano*, 2011, **5**, 5202-5213.
- 33 M. Ding, N. Song, X. He, J. Li, L. Zhou, H. Tan, Q. Fu and Q. Gu, *ACS Nano*, 2013, **7**, 1918-1928.
- 34 L. Zhou, D. Liang, X. He, J. Li, H. Tan, J. Li, Q. Fu and Q. Gu, *Biomaterials*, 2012, **33**, 2734-2745.
- 35 M. Ding, J. Li, X. He, N. Song, H. Tan, Y. Zhang, L. Zhou, Q. Gu, H. Deng and Q. Fu, *Adv. Mater.*, 2012, **24**, 3639-3645.
- 36 N. Song, M. Ding, Z. Pan, J. Li, L. Zhou, H. Tan and Q. Fu, *Biomacromolecules*, 2013, **14**, 4407-4419.
- 37 M. Ding, J. Li, X. Fu, J. Zhou, H. Tan, Q. Gu and Q. Fu, *Biomacromolecules*, 2009, **10**, 2857-2865.
- 38 (a) M. Ding, L. Zhou, X. Fu, H. Tan, J. Li and Q. Fu, *Soft Matter*, 2010, **6**, 2087-2092.; (b) M. Ding, X. He, Z. Wang, J. Li, H. Tan, H. Deng, Q. Fu and Q. Gu, *Biomaterials*, 2011, **32**, 9515-9524.; (c) M. Ding, X. He, L. Zhou, J. Li, H. Tan, X. Fu and Q. Fu, *J. Controlled Release*, 2011, **152**, e87-e89.; (d) M. Ding, J. Li, H. Tan and Q. Fu, *Soft Matter*, 2012, **8**, 5414-5428.
- 39 H. Tan, Z. Wang, J. Li, Z. Pan, M. Ding and Q. Fu, *ACS Macro Lett.*, 2013, **2**, 146-151.
- 40 C. B. Wang and S. L. Cooper, *Macromolecules*, 1983, **16**, 775-786.
- 41 J. A. Miller, S. B. Lin, K. K. S. Hwang, K. S. Wu, P. E. Gibson and S. L. Cooper, *Macromolecules*, 1985, **18**, 32-44.
- 42 (a) M. Wilhelm, C. Zhao, Y. Wang, R. Xu and M. A. Winnik, *Macromolecules*, 1991, **24**, 1033-1040.; (b) I. Astafieva, X. F. Zhong and A. Eisenberg, *Macromolecules*, 1993, **26**, 7339-7352.
- 43 (a) Y. Hu, X. Jiang, Y. Ding, L. Zhang, C. Yang, J. Zhang, J. Chen and Y. Yang, *Biomaterials*, 2003, **24**, 2395-2404.; (b) F. Quaglia, L. Ostacolo, G. De Rosa, M. I. La Rotonda, M. Ammendola, G. Nese, G. Maglio, R. Palumbo and C. Vauthier, *Int J Pharm*, 2006, **324**, 56-66.
- 44 (a) J. Du, T. Sun, W. Song, J. Wu and J. Wang, *Angew. Chem., Int. Ed.*, 2010, **49**, 3621-3626.; (b) Y. Huang, Z. Tang, X. Zhang, H. Yu, H. Sun, X. Pang and X. Chen, *Biomacromolecules*, 2013, **14**, 2023-2032.
- 45 (a) M. J. Hwang, J. M. Suh, Y. H. Bae, S. W. Kim and B. Jeong, *Biomacromolecules*, 2005, **6**, 885-890.; (b) A. S. Mikhail and C. Allen, *Biomacromolecules*, 2010, **11**, 1273-1280.
- 46 M. Ding, Z. Qian, J. Wang, J. Li, H. Tan, Q. Gu and Q. Fu, *Polym. Chem.*, 2011, **2**, 885-891.
- 47 A. Musacchio and E. D. Salmon, *Nat. Rev. Mol. Cell Bio.*, 2007, **8**, 379-393.